The current issue and full text archive of this journal is available at
www.emeraldinsight.com/0961-5539.htm

Optimally efficient multigrid algorithms for incompressible Euler equations

S.A. Mohamed
Department of Engineering Mathematics, Faculty of Engineering, Zagazig University, Zagazig, Egypt

Received 9 February 2007
Revised 6 June 2007
Accepted 29 June 2007

Abstract

Purpose – The aim of the paper is to achieve textbook multigrid efficiency for some flow problems.

Design/methodology/approach – The steady incompressible Euler equations are decoupled into elliptic and hyperbolic subsystems. Numerous classical FAS-MG algorithms are implemented and tested for convergence. A full multigrid algorithm that costs less than 10 work units (WUs) is sufficient to reduce the algebraic error below the discretization error. A new algorithm "NUVMGP" is introduced. A two-step iterative procedure is adopted. First, given the pressure gradient, the convection equations are solved on the computational grid for the velocity components by performing one Gauss-Seidel iteration ordered in the flow direction. second, a linear multigrid (MG) cycle for Poisson's equation is performed to update pressure values.

Findings – It is found that algorithm "NUVMGP-FMG" requires less than 6 WU to attain the target solution. The convergence rates are independent on both the mesh size and the approximation order.

Research limitations/implications – Lexicographic Gauss-Seidel using downstream ordering is a good solver for the advection terms and provides excellent smoothing rates for relaxation. But it is complicated to maintain downstream ordering in case the flow directions change with location.

Originality/value – Although the scope of this work is limited to rectangular domains, finite difference schemes, and incompressible Euler equation, the same approaches can be extended for other flow problems. However, such relatively simple problems may provide deep understanding of the ideal convergence behavior of MG and accumulate experience to detect unacceptable performance and regain the optimal one.

Keywords Fluid dynamics, Numerical analysis, Flow, Compressible flow

Paper type Research paper

1. Introduction

The multigrid (MG) approach is regarded as one of the most significant developments in numerical analysis in the last 30 years. MG techniques (Brandt, 1977, 1985; Hackbusch and Trottenberg, 1982; Briggs, 1987; Wesseling, 1992; Wesseling and Oosterlee, 2001) have proved to be among the fastest solvers for linear and nonlinear elliptic problems. The computational work required to solve a discrete problem containing N unknowns is O(N). Moreover, full multigrid (FMG) algorithms can solve a general discretized elliptic problem to the discretization accuracy in a computational work that is less than 10 work units (WUs), where a WU is the operation count in one residual evaluation on the computational grid. Such efficiency is known as textbook multigrid efficiency (TME) (Brandt, 1998).

Computational fluid dynamics (CFD) gives rise to very large systems requiring efficient solution methods. MG has contributed to many applications in CFD at an

International Journal of Numerical Methods for Heat & Fluid Flow
Vol. 18 No. 6, 2008
pp. 783-804

0961-5539
DOI 10.1108/09615530810885579

early stage. Over the years, MG has become closely intertwined with CFD, and has become an ingredient in major CFD codes. The viscous flow around a complete aircraft configuration and complex industrial flows in machinery are computed successfully with MG using its new features; adaptively, parallel computing, and unstructured grids.

However, full TME has not yet been achieved in realistic engineering applications in CFD in general. An important reason for this is that in CFD we often have to deal with singular perturbation problems. This gives rise to grids with cells having high-aspect ratios. Another reason is that the governing equations may show elliptic or parabolic behavior in one part of the domain and hyperbolic behavior in another part. This requires careful design of both the discretization and the solver. Therefore, extending TME to solutions of CFD equations is a challenging task (Brandt, 1998; Thomas *et al.*, 1999; Brandt *et al.*, 2002).

The TME methodology insists that each of the difficulties should be isolated, analyzed, and solved systematically using a carefully constructed series of model problems. According to Brandt (1985), one of the major obstacles to obtain better MG performance for advection-dominated flows is that the coarse grid provides only a fraction of the needed correction for smooth error components. This obstacle can be removed by designing a solver that effectively distinguishes between the elliptic, parabolic, and hyperbolic (advection) factors of the system and treats each one appropriately.

Recently, advanced MG flow solvers based on factorizable schemes have appeared and can be categorized into three approaches.

One approach to separate the factors is the distributed relaxation method proposed in Brandt (1985, 1998), Thomas *et al.* (1999), Brandt *et al.* (2002) and Diskin and Thomas (2003). Distributed relaxation introduces a set of auxiliary local variables. Using these variables, the relaxation equations form a triangular matrix with simple elliptic or hyperbolic terms on the main diagonal. Efficient relaxation of such factors is a much simpler task than relaxing the entire system of equations. The distributed relaxation is usually applied throughout the entire computational domain having the full effect away from boundaries in the regular flow field. The discrete equations near the boundaries are usually different from the interior equations due to the coupling of the relaxation equations near the boundaries. Diskin and Thomas (2003) presented an approach to the derivation of discretization schemes for which TME can be achieved by MG solvers with distributed relaxation. In particular, discrete schemes for the nonconservative Euler equations have been derived and analyzed and TME has been demonstrated in solving fully subsonic quasi-one-dimensional flow in a convergent/divergent channel.

Another approach was presented by Ta'asan (1994). This approach is based on a set of "canonical variables" which express the steady Euler equations in terms of elliptic and hyperbolic partitions. Ta'asan used this partition to guide the discretization of the equations. A staggered grid was used, with different variables residing at cell, vertex, and edge centers. In this reference, it was shown that ideal MG efficiency can be achieved for the compressible Euler equations for 2D subsonic flow using body fitted grids. One possible limitation of the use of the canonical variables is that the partition of the inviscid equations is not directly applicable to the viscous equations.

In the third approach (Roberts *et al.*, 1997, 2002; Mohamed *et al.*, 2005), a projection operator is applied to the incompressible Euler system of equations resulting in a Poisson equation for the pressure. Because the elliptic and advection parts of the system

are decoupled, ideal MG efficiency can be achieved. Compared to the distributive relaxation and the canonical variables' approaches, this method is extremely simple. A conventional vertex-based finite volume or finite difference discretization of the primitive variables was used, avoiding the need for staggered grids. This simplifies the restriction and prolongation operations, because the same operator can be used for all variables. The limitation of this approach, however, is that it is not clear if or not it can be generalized to the case of viscous compressible flows.

This approach was further generalized in Roberts *et al.* (2002) have combined this approach with the accurate global far-field artificial boundary conditions ABCs and computed the inviscid incompressible fluid flow around an airfoil. However, somewhat slower convergence was observed in the solution of the full Euler system compared with those obtained for pressure equation. This convergence deterioration was interpreted as a result of the following approximation. For the purpose of constructing the relaxation procedure for the full Euler system and due to the weak coupling between the pressure equation and the rest of the system, the right-hand side of Poisson's equation was considered as a subprincipal term and hence was disregarded.

A particular formulation of the scheme and corresponding MG algorithm that employ the factorization idea was proposed in Mohamed *et al.* (2005) which also contains more details concerning the implementation of the scheme and some numerical computations regarding the incompressible Euler equation discretized by first order finite difference scheme on a rectangular domain.

In this paper, we extend the work in Mohamed *et al.* (2005) by introducing a second order discretization scheme. However, our main contribution is to present a novel approach "NUVMGP" that proved to be optimally efficient. In contradiction with classical methods where the full Euler system is solved by MG, NUVMGP is an iterative procedure in which the convection equations are solved on the finest grid, for a given pressure gradient, by downstream Gauss-Seidel relaxation. Then the obtained velocity components are used to define the right-hand side of Poisson's equation, which is solved by a linear MG cycle. We intend to work out all the details (from theoretical issues to implementations) of many MG algorithms and then experimentally study the overall performance for a series of simple problems that allow for the direct comparison with the exact solution.

The rest of this paper is organized such that Section 2 presents the application of a projection of the differential operator of the Euler equation yielding a Poisson's equation for pressure in place of the continuity equation. The required additional boundary condition for pressure is derived from given boundary condition of the velocity components. The first- and second-order discretizations of the resulting system of differential equations are presented in Section 3. The details of the MG routines: relaxation, restriction, and prolongation as well as description of used MG algorithms including: V-, W-, FV-cycles, and the FMG algorithm are presented in Section 4. In Section 5, the new algorithm "NUVMGP" is presented. It applies Newton's method to solve the momentum equations for the velocity components u, v (for given pressure gradient) then solves Poisson's equation (with the right-hand side as function of given velocity) by MG for the pressure p. In Section 6, the robustness and efficiency of the proposed methods is demonstrated by presenting convergence analysis of the results obtained from solving the Euler equation on a rectangular domain where the exact

solutions are known for three different examples. Finally, conclusions are given in Section 7.

2. Formulation of the problem

The incompressible Euler equations in primitive variables in 2D are the two momentum equations in x-, y-directions and the continuity equation:

$$u\frac{\partial u}{\partial x}+v\frac{\partial u}{\partial y}+\frac{\partial p}{\partial x}=0,\quad u\frac{\partial v}{\partial x}+v\frac{\partial v}{\partial y}+\frac{\partial p}{\partial y}=0,\quad \frac{\partial u}{\partial x}+\frac{\partial v}{\partial y}=0, \tag{1}$$

where u, v are the components of the velocity in the x- and y-directions, respectively, and p is the pressure and the density is taken to be one.

Defining the advection operator as:

$$Q\equiv u\partial_x+v\partial_y, \tag{2}$$

where ∂_x, ∂_y are the partial differentiation operators, the Euler equations can be written as:

$$Lq=\begin{pmatrix} Q & 0 & \partial_x \\ 0 & Q & \partial_y \\ \partial_x & \partial_y & 0 \end{pmatrix}\begin{pmatrix} u \\ v \\ p \end{pmatrix}=0. \tag{3}$$

Introducing the operator Q^*, defined by:

$$Q^*(f)=-\partial_x(uf)-\partial_y(vf), \tag{4}$$

a projection operator R is defined as:

$$R=\begin{pmatrix} 1 & 0 & 0 \\ 0 & 1 & 0 \\ \partial_x & \partial_y & Q^* \end{pmatrix}. \tag{5}$$

Applying the projection operator to the Euler equations yields:

$$\tilde{L}q\equiv RLq=\begin{pmatrix} 1 & 0 & 0 \\ 0 & 1 & 0 \\ \partial_x & \partial_y & Q^* \end{pmatrix}\begin{pmatrix} Q & 0 & \partial_x \\ 0 & Q & \partial_y \\ \partial_x & \partial_y & 0 \end{pmatrix}\begin{pmatrix} u \\ v \\ p \end{pmatrix}=0, \tag{6}$$

or:

$$\begin{pmatrix} Q & 0 & \partial_x \\ 0 & Q & \partial_y \\ 0 & 0 & \Delta \end{pmatrix}\begin{pmatrix} u \\ v \\ p \end{pmatrix}+\begin{pmatrix} 0 \\ 0 \\ \partial_x Q(u)+Q^*(u_x)+\partial_y Q(v)+Q^*(v_y) \end{pmatrix}=0. \tag{7}$$

Simplifying the third row of the right matrix, Euler equations become:

$$\begin{pmatrix} Q & 0 & \partial_x \\ 0 & Q & \partial_y \\ 0 & 0 & \Delta \end{pmatrix} \begin{pmatrix} u \\ v \\ p \end{pmatrix} = \begin{pmatrix} 0 \\ 0 \\ 2u_x v_y - 2u_y v_x \end{pmatrix}. \tag{8}$$

The operator on the left-hand side of equation (8) is upper triangular. The pressure satisfies a Poisson equation for which a conventional relaxation method, such as Gauss-Seidel, can be applied. The momentum equations can be looked at as a standard advection equation with known pressure gradients and hence upwind differencing allows downstream relaxation to be used.

It is important to discuss the boundary conditions for the pressure. It is noticed that the order of equation (8) (second partial derivatives for p) is higher than the original system (1), where only first derivatives were required. Therefore, to ensure the well posedness of the problem, an extra boundary condition is essential. This additional boundary condition needs to be derived from the boundary conditions specified for the original problem and, possibly, differential equations of the original system.

2.1 Treating the boundary conditions on a rectangular grid

In case of a rectangular domain, the boundary conditions can be treated as follows. At a horizontal boundary $y = b$, if the velocity components $u(x, b)$ and $v(x, b)$ are known, then their x-derivatives u_x and v_x can be computed. So, p_y can be obtained using the second momentum and the continuity equation as follows:

$$p_y = -uv_x - vv_y = -uv_x + vu_x. \tag{9}$$

Similarly, at a vertical boundary $x = a$, if the velocity components $u(a, y)$ and $v(a, y)$ are known, then their y-derivatives u_y and v_y can be obtained and hence a boundary condition for pressure is derived using the first momentum and the continuity equation as follows:

$$p_x = -uu_x - vu_y = uv_y - vu_y. \tag{10}$$

The additional conditions for pressure associated with other arbitrary boundary conditions on even curved boundaries can be derived (Roberts *et al.*, 2002).

3. Discretization of Euler equations on a rectangle

Building the discrete system for the Euler equations by the finite difference method on a rectangular domain is considered and a uniform grid with mesh size h is assumed.

3.1 A first order scheme

The momentum equations are discretized using a standard first-order upwind-difference approximation to the advection operator and the pressure gradient. However, a second-order central-difference approximation is used to the Laplacian operator. The discrete system for the Euler equations (equation (8)) at an interior node (i, j) in a uniform mesh with mesh size h is given by:

$$\left.\begin{aligned} u_{i,j}\frac{u_{i,j}-u_{i-1,j}}{h}+v_{i,j}\frac{u_{i,j}-u_{i,j-1}}{h}+\frac{p_{i,j}-p_{i-1,j}}{h}&=0\\ u_{i,j}\frac{v_{i,j}-v_{i-1,j}}{h}+v_{i,j}\frac{v_{i,j}-v_{i,j-1}}{h}+\frac{p_{i,j}-p_{i,j-1}}{h}&=0\\ \frac{p_{i+1,j}+p_{i-1,j}+p_{i,j+1}+p_{i,j-1}-4p_{i,j}}{h^2}&=2\frac{u_{i,j}-u_{i-1,j}}{h}\cdot\frac{v_{i,j}-v_{i-1,j}}{h}-2\frac{u_{i,j}-u_{i,j-1}}{h}\cdot\frac{v_{i,j}-v_{i-1,j}}{h}\end{aligned}\right\}, \tag{11}$$

where $s_{i,j}$ is the s-variable at node (i, j). Thus, equation (11) is a system of three nonlinear algebraic equations in u, v, p at node (i, j) and some of its neighboring nodes. This equation has to be modified at boundaries appropriately. For example, at a lower horizontal boundary (Figure 1), if velocity components are specified, the value of p_y at that boundary is computed according to equation (9). The discrete form of this boundary condition is given by:

$$p_y = \frac{p_{i,j+1} - p_{i,j-1}}{2h}. \tag{12}$$

Equation (12) is used to substitute for the pressure at the ghost node $(i, j - 1)$ and the third equation in equation (11) reduces to:

$$\begin{aligned}\frac{p_{i+1,j}+p_{i-1,j}+2p_{i,j+1}-2h\cdot p_y-4p_{i,j}}{h^2} =& 2\frac{u_{i,j}-u_{i-1,j}}{h}\cdot\frac{v_{i,j}-v_{i,j-1}}{h}\\ &-2\frac{u_{i,j}-u_{i,j-1}}{h}\cdot\frac{v_{i,j}-v_{i-1,j}}{h}.\end{aligned} \tag{13}$$

3.2 A second order scheme

A second order upwind-difference approximation is obtained by substituting:

$$S_x = \frac{3S_{i,j} - 4S_{i-1,j} + S_{i-2,j}}{2h} \quad \text{or} \quad S_x = \frac{-3S_{i,j} + 4S_{i+1,j} - S_{i+2,j}}{2h},$$

according to the flow direction for a variable s. Here, s stands for u, v in the advection operator and the right-hand side of Poisson's equation and for p in the momentum equation. Thus, a second order discrete system for the Euler equations (equation (8)) at an interior node (i, j) is given by:

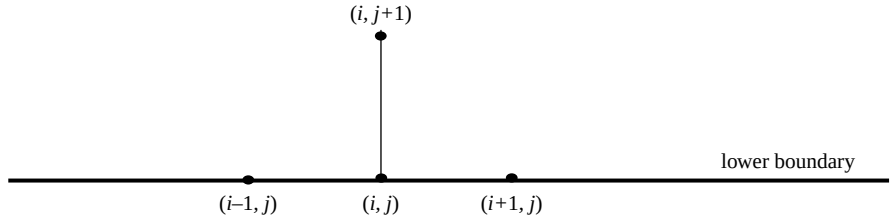

Figure 1.
Node (i, j) on a horizontal lower boundary

$$\left.\begin{aligned} u_{i,j}\frac{3u_{i,j}-4u_{i-1,j}+u_{i-2,j}}{2h}+v_{i,j}\frac{3u_{i,j}-4u_{i,j-1}+u_{i,j-2}}{2h}+\frac{3p_{i,j}-4p_{i-1,j}+p_{i-2,j}}{2h}=0\\ u_{i,j}\frac{3v_{i,j}-4v_{i-1,j}+v_{i-2,j}}{2h}+v_{i,j}\frac{3v_{i,j}-4v_{i,j-1}+v_{i,j-2}}{2h}+\frac{3p_{i,j}-4p_{i,j-1}+p_{i,j-2}}{2h}=0\\ \frac{p_{i+1,j}+p_{i-1,j}+p_{i,j+1}+p_{i,j-1}-4p_{i,j}}{h^2}=2\frac{3u_{i,j}-4u_{i-1,j}+u_{i-2,j}}{2h}\cdot\frac{3v_{i,j}-4v_{i,j-1}+v_{i,j-2}}{2h}\\ -2\frac{3u_{i,j}-4u_{i,j-1}+u_{i,j-2}}{2h}\cdot\frac{3v_{i,j}-4v_{i-1,j}+v_{i-2,j}}{2h}\end{aligned}\right\}. \tag{14}$$

4. The multigrid technique for solving Euler equations

The FAS MG technique will now be implemented for solving the discretized Euler equations. For convenience, first order discretization equations (equation (12)) are used to describe the relaxation scheme. Application of the same approach to the second order scheme (14) is straightforward. The main components of a MG V-cycle will be discussed in details.

A basic step in developing an efficient MG algorithm is to design an efficient relaxation procedure. For nonlinear problems, the relaxation updates to a current solution approximation are usually computed through Newton iterations. The full Newton linearization is a complicated operator, and its solution is expensive. Instead, the principal linearization is adopted here (Hackbusch and Trottenberg, 1982). The discretized highest derivative terms are considered principal and only their updates are considered through relaxation.

Superscripts are used to distinguish between the variables that will be updated in a current iteration m, and those that will be substitute their values from the previous iteration $m-1$. But according to the point-wise relaxation in the downstream direction, the values of u, v, and p at locations $(i, j-1)$ and $(i-1, j)$ would have been modified, then the first order discrete system is linearized as:

$$\left.\begin{aligned} u_{i,j}^{m-1}\frac{u_{i,j}^{m}-u_{i-1,j}^{m}}{h}+v_{i,j}^{m-1}\frac{u_{i,j}^{m}-u_{i,j-1}^{m}}{h}+\frac{p_{i,j}^{m-1}-p_{i-1,j}^{m}}{h}=0\\ u_{i,j}^{m-1}\frac{v_{i,j}^{m}-v_{i-1,j}^{m}}{h}+v_{i,j}^{m-1}\frac{v_{i,j}^{m}-v_{i,j-1}^{m}}{h}+\frac{p_{i,j}^{m-1}-p_{i,j-1}^{m}}{h}=0\\ \frac{p_{i+1,j}^{m-1}+p_{i-1,j}^{m}+p_{i,j+1}^{m-1}+p_{i,j-1}^{m}-4p_{i,j}^{m}}{h^2}=2\left(\frac{u_{i,j}^{m-1}-u_{i-1,j}^{m}}{h}\cdot\frac{v_{i,j}^{m-1}-v_{i,j-1}^{m}}{h}-\frac{u_{i,j}^{m-1}-u_{i,j-1}^{m}}{h}\cdot\frac{v_{i,j}^{m-1}-v_{i-1,j}^{m}}{h}\right)\end{aligned}\right\}. \tag{15}$$

For the purpose of relaxation, at the point (i, j), the first- and second-momentum equations are used for updating the u- and v-velocity components, and the Poisson equation is used for updating the pressure. In addition, to design a relaxation scheme for all grids, general right-hand sides are introduced and equation (15) is rearranged as:

$$\left.\begin{aligned} u_{i,j}^{m}&=\frac{\left(\mathrm{FU}_{i,j}\cdot h+u_{i,j}^{m-1}\cdot u_{i-1,j}^{m}+v_{i,j}^{m-1}\cdot u_{i,j-1}^{m}-p_{i,j}^{m-1}+p_{i-1,j}^{m}\right)}{\left(u_{i,j}^{m-1}+v_{i,j}^{m-1}\right)}\\ v_{i,j}^{m}&=\frac{\left(\mathrm{FV}_{i,j}\cdot h+u_{i,j}^{m-1}\cdot v_{i-1,j}^{m}+v_{i,j}^{m-1}\cdot v_{i,j-1}^{m}-p_{i,j}^{m-1}+p_{i,j-1}^{m}\right)}{\left(u_{i,j}^{m-1}+v_{i,j}^{m-1}\right)}\\ p_{i,j}^{m}&=\frac{\left(p_{i+1,j}^{m-1}+p_{i-1,j}^{m}+p_{i,j+1}^{m-1}+p_{i,j-1}^{m}-\mathrm{FP}_{i,j}\cdot h^2\right)}{4}\end{aligned}\right\}, \tag{16}$$

where, for the computational grid:

$$\mathrm{FU}_{i,j} = 0, \quad \mathrm{FV}_{i,j} = 0,$$
$$\mathrm{FP}_{i,j} = 2\left(\frac{u_{i,j}^{m-1} - u_{i-1,j}^{m}}{h} \cdot \frac{v_{i,j}^{m-1} - v_{i,j-1}^{m}}{h} - \frac{u_{i,j}^{m-1} - u_{i,j-1}^{m}}{h} \cdot \frac{v_{i,j}^{m-1} - v_{i-1,j}^{m}}{h}\right). \tag{17}$$

On the other hand, $\mathrm{FU}_{i,j}$, $\mathrm{FV}_{i,j}$, $\mathrm{FP}_{i,j}$ are computed on coarser grids through the FAS restriction subroutine.

The Gauss-Seidel relaxation is applied in lexicographic order in the downstream direction. So this order is dependent on the boundary conditions. Downstream marching is a very efficient solver that yields an accurate solution to a nonlinear hyperbolic equation. For the convection terms in the momentum equations, a single downstream sweep provides the exact solution to the linearized problem (first and second equations in equation (15)) if the pressure gradient is exact.

It is important to notice that while equation (15) is used for computing relaxation updates, the original formulation (13), with appropriate right-hand sides, is used for computing residuals. Two methods of restriction are implemented in this work; the trivial injection operator for the solution and the full-weighting operator for the residual. For the prolongation, bilinear interpolation operator is adopted.

5. Multigrid basics and algorithms

First, we present a brief description of MG principles. To establish notation and terminology, we start by formulating the basic two-grid algorithm. Consider a system of m partial differential equations on a domain Ω discretized by a grid G^h. The resulting nonlinear algebraic system is denoted as:

$$N^h(u^h) = b^h. \tag{18}$$

Let there also be a coarse grid $G^H \subset G^h$ with fewer nodes than G^h. Let its discrete system be:

$$N^H(u^H) = b^H. \tag{19}$$

5.1 The nonlinear full approximation scheme (FAS) multigrid method

The basic two-grid algorithm is given by:

Repeat until convergence:

begin

(1) $S\nu_1\left(u_0^h; u_{1/3}^h, b^h\right); \quad r^h = b^h - N\left(u_{1/3}^h\right);$

(2) restrict $u_{1/3}^h$ and r^h; $b^H = N^H\left(\widehat{R}\,u_{1/3}^h\right) + Rr^h;$

(3) solve $\left(u_{1/3}^H; u_{2/3}^H, b^H\right);$

(4) $u_{2/3}^h = u_{1/3}^h + P\left(u_{2/3}^H - u_{1/3}^H\right);$

(5) $S\nu_2\left(u_{2/3}^h; u_1^h, b^h\right);$

(6) $u_0^h = u_1^h;$

end.

Step (1) (pre-smoothing) consists of ν_1 relaxations with some iterative method for the fine grid equation (18) with initial iterate u_0^h and result $u_{1/3}^h$ and computation of the residual r^h. In Step (2), $\widehat{R}$ is the fine to coarse grid restriction operator for variables such that $u_{1/3}^H = \widehat{R} u_{1/3}^h$ while R is restriction operator for residuals that need not be the same as $\widehat{R}$. In Step (3), the coarse grid problem is solved approximately by some iteration method. In Step (4), the coarse grid correction is added to the current fine grid iterate. Here, P is a prolongation. In Step (5), post-smoothing takes place by performing ν_2 relaxations on the fine grid.

5.2 MG cycles and algorithms

The MG method is obtained if solution of the coarse grid problem in Step (3) is replaced by γ iterations with the two-grid method, employing a still coarser grid, and so on, until the coarsest grid is reached, where the problem is solved exactly. With $\gamma = 1$ or $\gamma = 2$, the V- or W-cycle is obtained, respectively.

Both the V- and W-cycles are shown in Figure 2 for a computational grid G_4 and three coarser grids. The number of relaxations on the downward and upward legs of the cycles are denoted by ν_1 and ν_2, respectively, with $\nu_3 = \nu_1 + \nu_2$. Also shown another cycle termed the FV-cycle (Thomas *et al.*, 1999) and a representation of the FMG algorithm.

To estimate the computational work for different cycles, a WU is defined as the operation count required to complete one relaxation sweep on the finest grid.

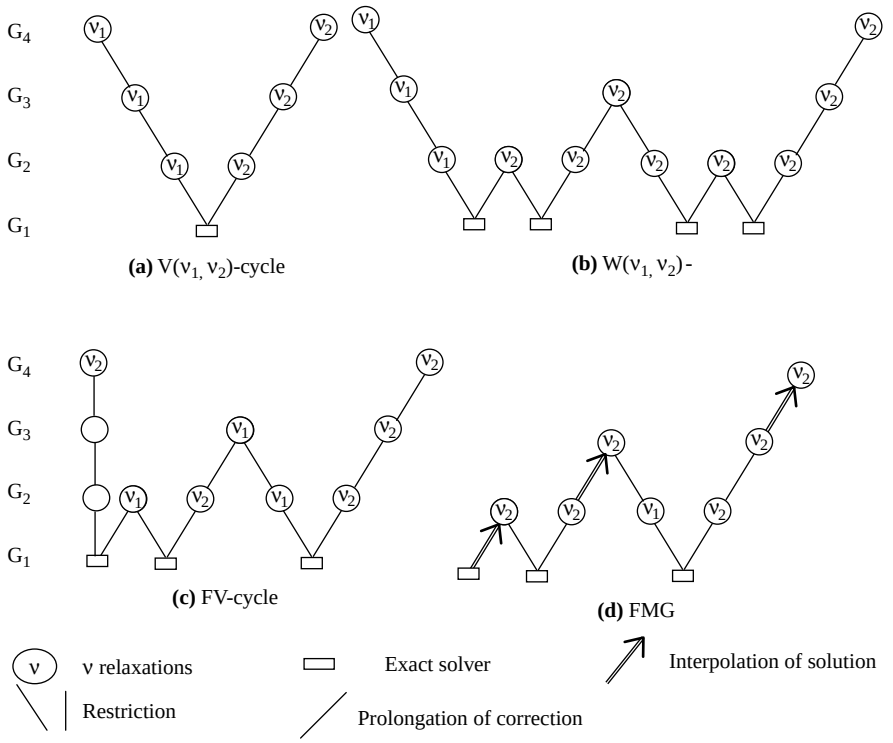

Figure 2.
Different MG cycles and algorithms

A relaxation on the next coarser grid costs 1/4 WU in 2D and for mesh size ratio $H/h = 2$. Thus, one can easily estimate, in the limit of an infinite number of levels, the computational work required for different cycles. Some of these estimates are summarized in Table I.

In general, few MG cycles are sufficient to reduce the algebraic error norm of the discrete system below the truncation error norm. However, starting the computations by performing FMG procedure provides a good initial approximation for the solution especially for nonlinear problems. In an FMG, the problem is solved on the coarsest grid and the solution is interpolated to the next fine grid that can be solved approximately by performing one V-cycle, and so on until the finest grid.

5.3 The two-steps iterative procedure – "NUVMGP" algorithm

The idea behind this algorithm was motivated by the following two observations. First, when the momentum equations were solved on a computational grid for the velocity components given the exact values for pressure, excellent results were obtained by Newton's iterations and also by the lexicographic Gauss-Seidel iterations. One or two iterations were sufficient to obtain the exact solution. Second, it was observed that the convergence rates of the MG cycles for the Euler's equations were not as good as those rates of Poison's equation. This can be understood because the third equation in Euler's system is Poisson-like equation because its left-hand side is not a known function but dependent on the current values of the velocity components. Substituting exact values of velocity, the Euler system is solved by MG with ideal convergence rates.

To regain the correspondence between equations and unknowns, let the Euler's system (equation (8)) be rewritten in the form of the following two subsystems:

$$\begin{pmatrix} Q & 0 \\ 0 & Q \end{pmatrix} \begin{pmatrix} u \\ v \end{pmatrix} = \begin{pmatrix} -\bar{p}_x \\ -\bar{p}_y \end{pmatrix}, \tag{20}$$

$$\Delta p = 2\bar{u}_x\bar{v}_y - 2\bar{u}_y\bar{v}_x, \tag{21}$$

where Q is defined by equation (2) and an over bared variable corresponds to a good approximation value of that variable. Given the pressure gradient in the right-hand side of equation (20), then the first subsystem is associated with the velocity components. In addition, given the velocity gradients, equation (21) is associated to the pressure.

In the proposed iterative two-steps algorithm "NUVMGP", an iteration corresponds to a cycle and consists of two-steps. The first step is to use Newton's method to solve equation (20), on the computational grid, for u and v. Then as a second step, MG solves equation (21) for p. Two Newton's iterations are required to obtain accurate solution to

Cycle	Cost (ν_1, ν_2)	Cost (2, 1)
V-cycle	$(\nu_1 + \nu_2)\left(1 + \frac{1}{4} + \frac{1}{4^2} + \frac{1}{4^3} + \cdots\right) = \frac{4}{3}(\nu_1 + \nu_2)$	4
FV-cycle	$2\nu_2 + (\nu_1 + \nu_2)\left(\frac{1}{4} + \frac{2}{4^2} + \frac{3}{4^3} + \cdots\right) = 2\nu_2 + \frac{4}{9}(\nu_1 + \nu_2)$	10/3
FMG	$\nu_2\left(1 + \frac{1}{4} + \frac{1}{4^2} + \cdots\right) + (\nu_1 + \nu_2)\left(\frac{1}{4} + \frac{2}{4^2} + \frac{3}{4^3} + \cdots\right) = \frac{4}{3}\,\nu_2 + \frac{4}{9}(\nu_1 + \nu_2)$	8/3

Table I.
Estimated computational work for different cycles represented in Figure 2

the nonlinear subsystem equation (20). However, if a good initial guess is provided for u and v, as would be the case when FMG is applied, one Gauss-Seidel relaxation is sufficient to solve equation (20). With respect to Poisson's equation, equation (21), only one MG V-cycle is required. Figure 3 shows a representation for a "NUVMGP" cycle, where G_4 is the computational grid. The computational cost for this cycle is estimated as follows. If a relaxation sweep of the full Euler's system (three equations) costs one WU then a reasonable estimation of the costs of a relaxation for equations (20) and (21) are 2/3 and 1/3 WU, respectively. Thus, the cost of a "NUVMGP" cycle is:

$$\frac{2}{3}+\frac{1}{3}(\nu_1+\nu_2)\left(1+\frac{1}{4}+\frac{1}{16}+\frac{1}{64}+\cdots\right)=\frac{2}{3}+\frac{4}{9}(\nu_1+\nu_2)\ \text{WUs}.$$

If, $\nu_1 = 2$ and $\nu_2 = 1$, "NUVMGP" cycle costs 2 WU while the cost of the classical V(2,1)is 4 WU.

6. Numerical results

The objective of the numerical examples presented in this section is to emphasize the efficiency of the proposed discretizations, approaches and algorithms. The problem of inviscid flow over a rectangular domain is considered. Figures 2(a)-(c) show a square domain of unit length and boundary conditions for three different flows with known solutions that satisfy equation (1). It is easy to prove that these problems have the exact solutions:

$$\text{(a)}\ \ u = e^{y}, \quad \nu = e^{x}, \quad p = -e^{x+y}, \tag{22}$$

$$\text{(b)}\ \ u = x + 2, \quad \nu = 2 - y, \quad p = \frac{-(x^2+y^2)}{2-2x+2y}, \tag{23}$$

$$\text{(c)}\ \ u = \sin x\ \sin y, \quad \nu = \cos x\ \cos y, \quad p = \frac{-(\sin^2 x+\cos^2 y)}{2}. \tag{24}$$

The domain is discretized by nested sequence of uniform grids with mesh sizes $h = (1/2^{\ell}), \quad \ell = 1, 2, \ldots, L$. For the coarsest grid G_1, $h = 1/2$, the grid has nine

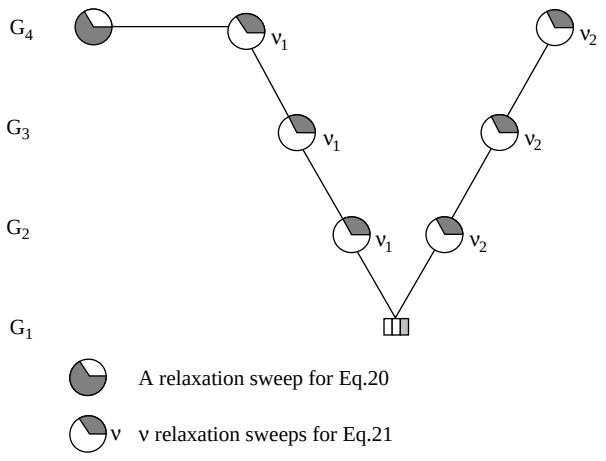

Figure 3.
A representation of "NUVMGP" cycle

nodes while on the finest grid, $h = 1/2^L$, there are $(2^L + 1)^2$ nodes. The ordering of the grid vertices was from the lower-left to the upper-right of the domain such that a lexicographic Gauss-Seidel relaxation results in downstream ordering.

6.1 Convergence analysis for different discretization schemes

Both of the first- and second-order discretization schemes, described in Section 3, were implemented in a FAS_V(2,1) MG cycle. That is, two relaxation sweeps are performed on each grid before restriction to a coarser grid, and one relaxation sweep is performed after prolongation to a fine grid. Thus, a single V(2,1) cycle costs approximately 4 WU. The main objective here is to discuss the convergence behavior of this cycle based on both of the algebraic error and discretization error.

The algebraic error is defined as the difference between the exact and approximate solutions of the discrete problem. Practically, residual produced when the approximate solution is substituted into the discrete system is computed rather than the algebraic error since the exact solution of the algebraic system is generally unknown. On the other hand, a fast residual convergence is considered to be an important monitoring tool for the algebraic error.

The MG V(2,1)-cycle is used to solve the inviscid flow model problems (Figure 4) on uniform computational grids G_5, G_6, G_7, and G_8, with mesh sizes $h = 1/32$, 1/64, 1/128, and 1/256, respectively. After each cycle, the L_2- residual norm is computed for u, v, and p.

In this subsection, we will present the results of problem (1), with boundary conditions shown in Figure (4a) and exact solution given by equation (21). Also we will discuss only the convergence behavior of the pressure p since similar behaviors were obtained for u and v. For each computational grids G_L, $L = 5, 6, 7$, and 8, the results of the L_2 residual norm after each of ten V-cycles are summarized in Table II for the first- and second-discretization schemes. The last two rows in the table contain the average residual reduction per cycle in the first ten- and four-cycles denoted by μ(1-10) and μ(1-4), respectively. One can easily conclude that the convergence rate is comparable with those rates ($\mu = 0.125$) of the V(2,1) cycle when applied to Poisson's equation. However, the convergence rate is not uniform. These rates are better in the first four cycles. Another important observation is that the convergence rates are independent of the mesh size h and the discretization scheme. Also it is noted that the residual norm converges to the computational zero, or equivalently, it vanishes to the round-off error level.

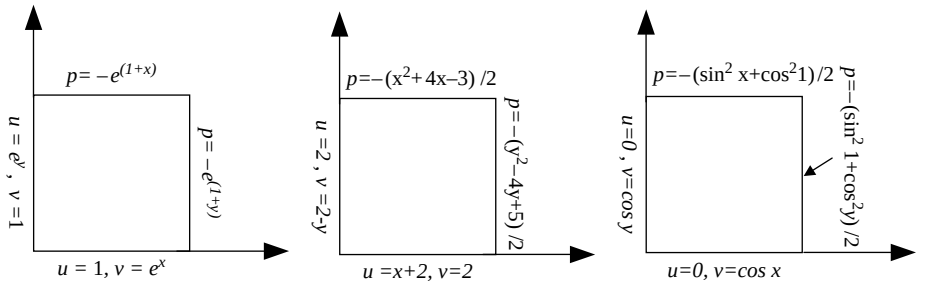

(a) Problem 1 **(b)** Problem 2 **(c)** Problem 3

Figure 4.
The domain and boundary conditions of the three model problems

Cycles	First-order scheme				Second-order scheme			
	$L = 5$	$L = 6$	$L = 7$	$L = 8$	$L = 5$	$L = 6$	$L = 7$	$L = 8$
0	1.27×10^{3}	3.55×10^{3}	1.00×10^{4}	2.82×10^{4}	1.27×10^{3}	3.55×10^{3}	1.00×10^{4}	2.82×10^{4}
1	3.37×10^{1}	9.07×10^{1}	2.49×10^{2}	6.92×10^{2}	3.37×10^{1}	9.07×10^{1}	2.49×10^{2}	6.92×10^{2}
2	1.57	4.40	1.21×10^{1}	3.33×10^{1}	1.54	4.38	1.21×10^{1}	3.33×10^{1}
3	2.79×10^{-1}	4.40×10^{-1}	7.96×10^{-1}	1.81	3.25×10^{-1}	4.75×10^{-1}	8.25×10^{-1}	1.85
4	4.58×10^{-2}	7.20×10^{-2}	1.02×10^{-1}	1.47×10^{-1}	5.48×10^{-2}	8.11×10^{-2}	1.09×10^{-1}	1.52×10^{-1}
5	1.77×10^{-2}	2.72×10^{-2}	3.80×10^{-2}	4.75×10^{-2}	2.18×10^{-2}	3.11×10^{-2}	4.09×10^{-2}	4.93×10^{-2}
6	3.42×10^{-3}	5.99×10^{-3}	9.67×10^{-3}	1.30×10^{-2}	4.37×10^{-3}	7.39×10^{-3}	1.09×10^{-2}	1.38×10^{-2}
7	1.23×10^{-3}	2.08×10^{-3}	3.24×10^{-3}	4.34×10^{-3}	1.63×10^{-3}	2.58×10^{-3}	3.68×10^{-3}	4.64×10^{-3}
8	2.43×10^{-4}	4.54×10^{-4}	8.28×10^{-4}	1.20×10^{-3}	3.23×10^{-4}	6.17×10^{-4}	9.85×10^{-4}	1.31×10^{-3}
9	8.50×10^{-5}	1.60×10^{-4}	2.81×10^{-4}	4.03×10^{-4}	1.20×10^{-4}	2.15×10^{-4}	3.34×10^{-4}	4.41×10^{-4}
10	1.71×10^{-5}	3.53×10^{-5}	7.44×10^{-5}	1.16×10^{-4}	2.38×10^{-5}	5.31×10^{-5}	9.32×10^{-5}	1.30×10^{-4}
μ(1-10)	0.1633	0.1584	0.1539	0.14502	0.1688	0.1650	0.1574	0.1467
μ(1-4)	0.0775	0.0671	0.0566	0.0478	0.0810	0.0691	0.0575	0.0482

Table II.
Residual norm of MG-V(2,1) cycles for first- and second-schemes

The same results are shown in Figure 5(a) and (b) for the first- and second-discretization schemes, respectively. The convergence behavior of the Poisson's equation, that resulted when the exact values of u and v were substituted in the Euler system, is shown in Figure 5(b). It is observed that the convergence rate of the MG cycles is more uniform for this case. However, it can be concluded that the average convergence rate is the same for both the full Euler system and the Poisson's equation (Figure 5(b)). This optimal convergence rate was not obtained in Roberts *et al.* (2002) where slower convergence was observed in the solution of the full Euler system compared with those obtained for pressure equation. A reasonable interpretation was given by the authors that this convergence deterioration results due to disregarding subprincipal terms in the relaxation scheme.

In reality, the objective of MG algorithms is fast convergence to the solution of the differential equations, not necessarily fast asymptotic residual convergence. The natural solution tolerance is the discretization error.

The discretization error is defined as the difference between the exact solutions of discrete and differential problems. To discuss the behavior of the proposed algorithm and since the exact solution is known (equation (21)), the L_2-norm of the difference between computed solution after each cycle and the exact solution of the differential system is calculated for the pressure and summarized in Table III, and also in Figure 6(a) and (b) using the first- and second-order discretization schemes, respectively. These results are presented for different computational grids with mesh sizes $h = 1/32, 1/64, 1/128, 1/256$ on computational grids G_L, $L = 5, 6, 7$, and 8, respectively.

It is observed that, for a given computational grid G_L, this computed norm decreases uniformly through the first few cycles (four to ten cycles) then remains unchanged at some value ε_L corresponding to the discretization error at this grid. This means that excess computation does not increase the desired accuracy. This is because the exact solution of the discrete system has been reached (within algebraic error less than the discretization error) after these few cycles.

It is observed (Table III) that the discretization error norm depends on both the mesh size h and the order of approximation. To discuss this dependency, the values of $\varepsilon_L/\varepsilon_{L-1}$ are computed and reported in the last row of Table III for different grids. For each of the first- and second-approximation schemes these values for all computational

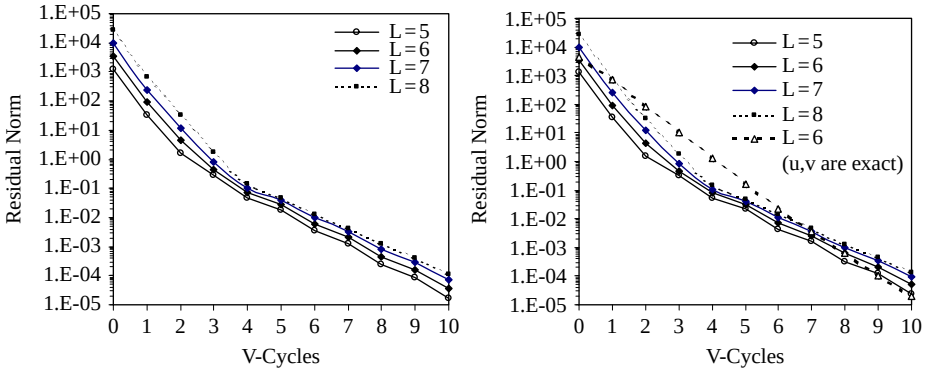

(a) First- order discretization scheme

(b) Second-order discretization scheme

Figure 5.
Convergence behavior of the residual norm

Cycles	First-order scheme				Second-order scheme			
	$L=5$	$L=6$	$L=7$	$L=8$	$L=5$	$L=6$	$L=7$	$L=8$
0	3.10	3.14	3.17	3.18	3.10	3.14	3.17	3.18
1	5.03×10^{-1}	4.99×10^{-1}	4.98×10^{-1}	4.97×10^{-1}	5.02×10^{-1}	4.99×10^{-1}	4.98×10^{-1}	4.97×10^{-1}
2	1.94×10^{-1}	1.83×10^{-1}	1.78×10^{-1}	1.75×10^{-1}	1.67×10^{-1}	1.69×10^{-1}	1.70×10^{-1}	1.71×10^{-1}
3	8.32×10^{-2}	7.27×10^{-2}	6.74×10^{-2}	6.47×10^{-2}	5.93×10^{-2}	6.01×10^{-2}	6.09×10^{-2}	6.15×10^{-2}
4	4.07×10^{-2}	2.82×10^{-2}	2.17×10^{-2}	1.85×10^{-2}	1.60×10^{-2}	1.52×10^{-2}	1.51×10^{-2}	1.52×10^{-2}
5	3.05×10^{-2}	1.80×10^{-2}	1.16×10^{-2}	8.47×10^{-3}	6.38×10^{-3}	5.31×10^{-3}	5.17×10^{-3}	5.21×10^{-3}
6	2.71×10^{-2}	1.43×10^{-2}	7.74×10^{-3}	4.44×10^{-3}	2.97×10^{-3}	1.59×10^{-3}	1.26×10^{-3}	1.19×10^{-3}
7	2.63×10^{-2}	1.35×10^{-2}	6.99×10^{-3}	3.71×10^{-3}	2.26×10^{-3}	8.49×10^{-4}	5.13×10^{-4}	4.39×10^{-4}
8	2.61×10^{-2}	1.32×10^{-2}	6.68×10^{-3}	3.39×10^{-3}	2.01×10^{-3}	5.64×10^{-4}	2.02×10^{-4}	1.13×10^{-4}
9	2.60×10^{-2}	1.32×10^{-2}	6.63×10^{-3}	3.34×10^{-3}	1.96×10^{-3}	5.14×10^{-4}	1.52×10^{-4}	6.21×10^{-5}
10	2.60×10^{-2}	1.32×10^{-2}	6.61×10^{-3}	3.31×10^{-3}	1.94×10^{-3}	4.92×10^{-4}	1.28×10^{-4}	3.60×10^{-5}
		0.508	0.501	0.501		0.254	0.260	0.281

Table III.
Discretization error for first- and second-schemes on different grids

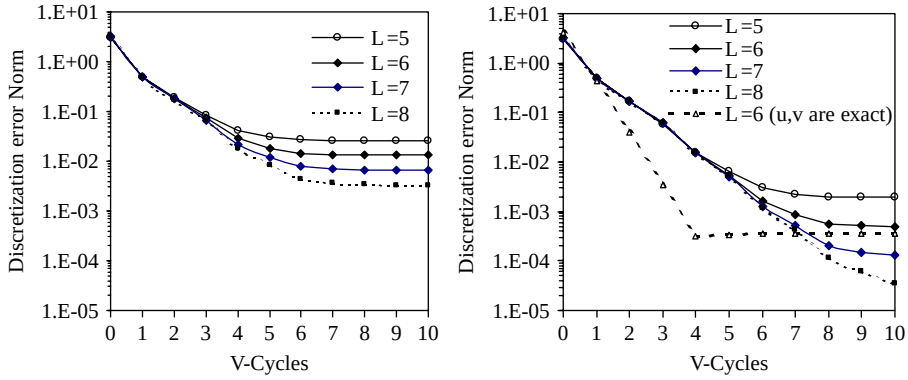

(a) First- order discretization scheme

(b) Second-order discretization scheme

Figure 6.
Convergence behavior of the discretization error norm

grids are nearly constant and equal to 1/2 and 1/4, respectively, which is the theoretical orders of approximations (O(h), O(h^2)).

To compare convergence behavior of the MG V-cycles for the Euler's system to attain the discretization error norm with that for Poisson's equation, the same results were obtained for Euler's system on the computational grid G_6 but after substituting the exact values for the velocity components. This substitution reduces the Euler's system to the scalar Poisson's equation. The obtained results are plotted in Figure 6(b) showing ideal convergence rate and slightly less discretization error. This can be understood since the third equation in Euler's system, equation (20), differs from Poisson equation in that its right-hand side is dependent on the velocity components.

6.2 Convergence analysis for different cycles

In this study, problem (1) is solved on computational grid G_6 using different cycles, namely the V(2,1), W(2,1), and NUVMGP-V(2,1)cycles. Results of the L_2 residual norms and discretization error norms for u, v, and p are computed after each of ten cycles and shown in Figure 7(a) and (b) for the velocity components and for p, respectively. The first observation is the similar convergence behaviors of each cycle for the velocity components and pressure. It is also observed that although the convergence of the residual norm is better for the V-cycle than that of the W-cycle, their convergence to the discretization error is identical. Finally, one can easily conclude that NUVMGP-V-cycle is the most efficient one. It has the same convergence behavior of the classical V-cycle but it costs approximately half the computations required for the V-cycle as discussed in the previous section.

To demonstrate the robustness of NUVMGP-V cycle, its convergence behavior for residual norms and to the discretization error is plotted for different computational grids in Figure 8(a) and (b) for the pressure and velocity components, respectively.

It is noticed that no plots were shown for the residual norm of the velocity components in Figures 7(a) and 8(b). That is simply because in the NUVMGP algorithm, each cycle represents an iteration that consists of two steps. The first is the solution of the momentum system for the velocity components, given the current pressure gradient, on the computational grid. This solution process results in trivial

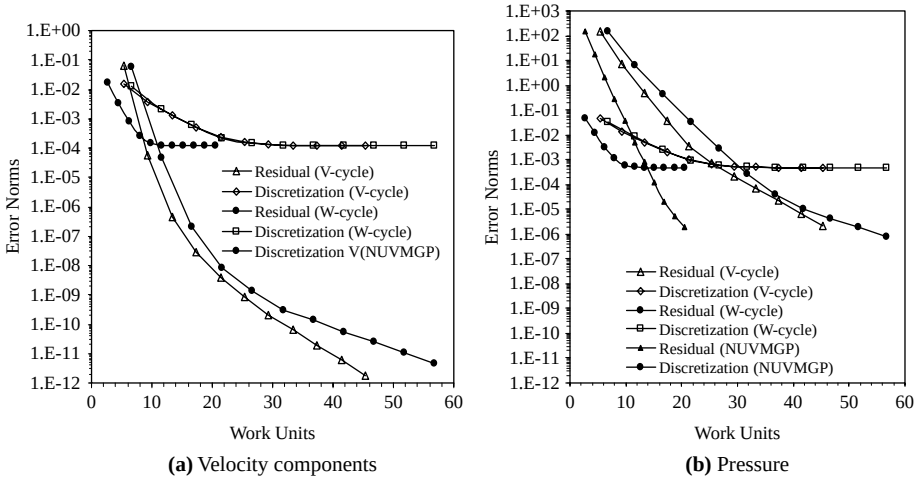

(a) Velocity components **(b)** Pressure

Figure 7. Convergence history of residual and discretization norms for V-, W-, and NUVMGP-V cycles

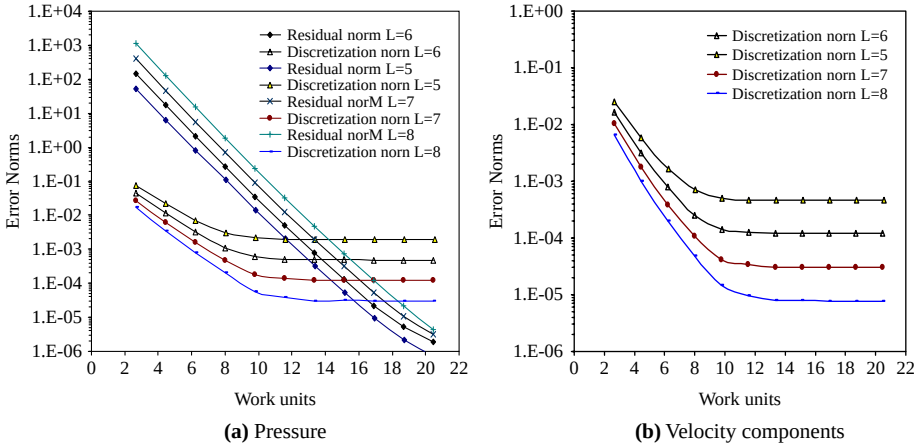

(a) Pressure **(b)** Velocity components

Figure 8. NUVMGP-V cycles convergence on different computational grids

residual for the current system. The second step is approximating the pressure by performing a V-cycle for the Poisson's equation.

6.3 The full multigrid (FMG) algorithm

The cycling algorithms presented and tested in previous sections are easily converted into FMG programs. The main difference is that instead of starting with an arbitrary approximation on the finest grid, the first approximation is provided by an interpolation from a coarse-grid solution. A representation of FMG is shown in Figure 2(d) for a computational grid G_4 and three coarser grids. The FMG is implemented using a bilinear interpolation routine as well as the V-cycle routines. Although the computational cost of FMG is approximately equal to that of a single V-cycle, it reduces the algebraic error of the discrete system and hence less number of V-cycles is required. The performance of the V(2,1)-cycling starting with and without FMG is shown in Figure 9. In Figure 9(a)

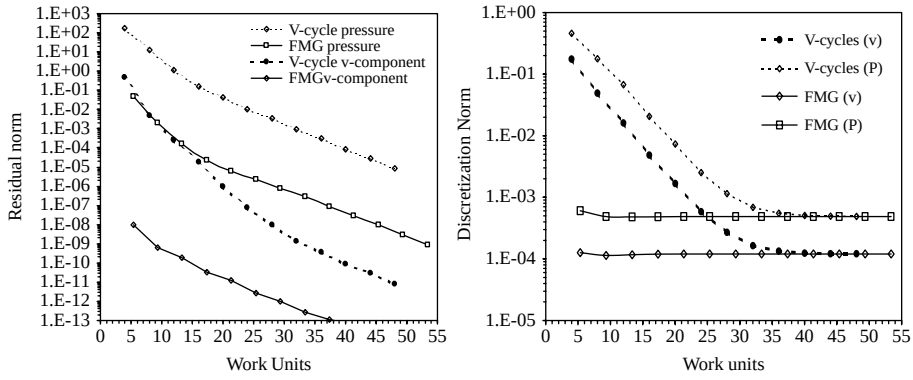

Figure 9.
Convergence behavior of FMG and V-cycles for velocity component (v) and pressure (p)

the L_2 residual norm is plotted for the velocity components and pressure. A considerable reduction in the initial residual norm is observed when starting the cycling by performing FMG then due to the same convergence behavior of the next V-cycles, the two curves seem to be parallel. In Figure (9b), the L_2 norm of the difference between the exact and computed solutions after each cycle is plotted. Starting by FMG provides excellent results. Only one V-cycle is required to reach the discretization error level costing less than 10 WU compared with 40 WU required for the classical V-cycling.

6.4 FMG-NUVMGP algorithm

It is expected that combining FMG and NUVMGP algorithms would result in an optimally efficient solver. First, the computational work of these methods will be discussed in some details. Since the FMG method acts on the full Euler's system (the three equations), it costs 8/3 WU (Table I). With respect to the NUVMGP-FV(2,1)-cycle, the cheap Gauss-Seidel relaxation is used in place of the Newton iteration for the solution of the two-momentum equations on the finest grid. This would cost 2/3 WU. According to the NUVMGP method, the FV(2,1)-cycle acts on only a single, Poisson's equation, rather than the full system and thus reduces its cost to one-third. Thus, the total cost of NUVMGP-FV(2,1)-cycle (Table I) is $2/3 + (10/3)/3 = 16/9$ WU.

To study the performance of such algorithm the FMG (Figure 2(d)) is implemented followed by 12 NUVMGP FV(2,1)-cycles to solve the problem on different grids G_L, $L = 5, 6, 7, 8$. The results are shown in Figure 10(a) for the residual norm versus WUs and prove the convergence of the residual norm for both velocity components v and pressure p to the computational zero. In Figure 10(b), the norm of the difference between the exact and computed solution of pressure p at the end of each cycle is plotted. It is important to notice the fast convergence to the discretization error. Only 6 WU (FMG then 2 FV(1,1) cycles) are sufficient to solve the problem. More important is that this cost is independent of the mesh size.

To demonstrate the effect of FMG in providing good approximation of the discrete system, the algebraic error is estimated as the difference between the computed solutions just after FMG and the exact one (obtained at the end of the 12 V-cycles). Also the discretization error is computed as the difference between the exact solutions of the continuous and discrete problems. These results are summarized in Table IV for

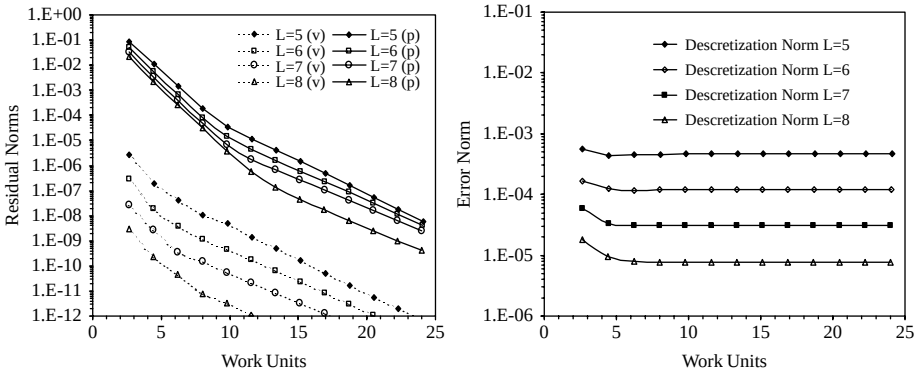

(a) Residual norm

(b) Discretization norm

Figure 10.
Convergence behavior of FMG-NUVMGP algorithm on different grids

	Discretization error norm		Algebraic/descretization error norms	
	v	p	v	p
$L = 5$ ($h = 1/32$)	4.61×10^{-4}	1.93×10^{-3}	8.19×10^{-2}	3.70×10^{-2}
$L = 6$ ($h = 1/64$)	1.20×10^{-4}	4.87×10^{-4}	7.97×10^{-2}	4.26×10^{-2}
$L = 7$ ($h = 1/128$)	3.07×10^{-5}	1.22×10^{-4}	1.35×10^{-1}	1.33×10^{-1}
$L = 8$ ($h = 1/256$)	7.75×10^{-6}	3.06×10^{-5}	2.46×10^{-1}	2.05×10^{-1}

Table IV.
Algebraic and discretization error norms after one FMG-NUVMGP cycle

different computational grids where discretization error norm and the ratio of the algebraic to discretization error norms are given for velocity components and pressure. The results demonstrate the ability of FMG to reduce the algebraic error below the discretization error.

6.5 Convergence rates for different problems

Although all results presented until now were obtained for problem (1), the other two problems in Figure 4 shows similar results. A sample comparison is shown in Figure 11, where the convergence behaviors of the residual norm and to the discretization error norm for the three problems are plotted for the velocity component v and pressure p. The FMG-NUVMGP approach is applied on computational grid G_6.

7. Conclusions

A MG method for solving the incompressible Euler equation has been developed by exploiting factorizability of the governing differential operator. Treating each of the factors appropriately, optimal convergence rates have been attained. First- and second-order discretization schemes are presented. No artificial viscosity is introduced in the discretization. Elements of the full approximation scheme MG algorithm, including relaxation, residuals, restriction, prolongation, cycling, and FMG routines are presented. A novel algorithm "NUVMGP" has been developed and proved to be optimally efficient. The convergence rates of the algebraic and discretization error are tested for different algorithms. The main conclusions are:

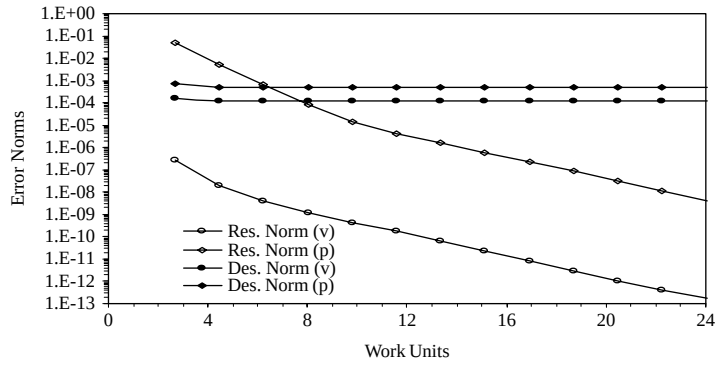

(a) Problem 1

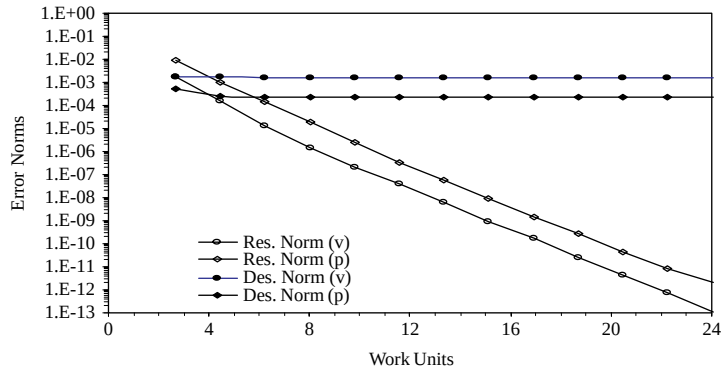

(b) Problem 2

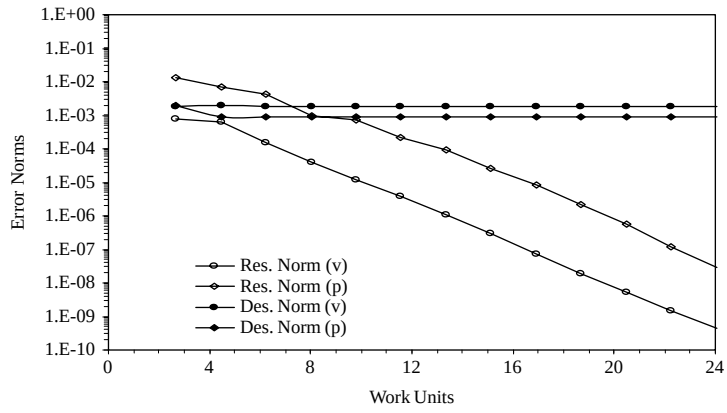

(c) Problem 3

Figure 11.
FMG-NUVMGP convergence behavior for different problems

- After few (four to ten) MG V(2,1)-cycles that cost (16-40 WU), the algebraic error is reduced substantially below the discretization error.
- Starting by FMG reduces the algebraic error below the discretization error making the target solution obtainable after one V-cycle (with total cost less than 10 WU).
- Algorithm "NUVMGP-V" consumes WUs less than half that required by classical V-cycle.
- Algorithm "NUVMGP-FMG" requires less than 6 WU to attain the target solution.
- The convergence rates of residual norm are independent of the mesh size and the approximation order.
- Lexicographic Gauss-Seidel using downstream ordering is a good solver for the advection terms and provides excellent smoothing rates for relaxation. But it is complicated to maintain downstream ordering in case the flow directions change with location.
- Although the scope of this work is limited to rectangular domains, finite difference schemes, and incompressible Euler equation, the TME is attained and even improved. Moreover, such relatively simple problems may provide deep understanding of the ideal convergence behavior of MG and accumulate experience to detect unacceptable performance and regain the optimal one.

References

Brandt, A. (1977), "Multi-level adaptive solutions to boundary-value problems", *J. Mathematics of Computation*, Vol. 31, pp. 333-90.

Brandt, A. (1985), "Multigrid techniques: 1984 guide with applications to fluid dynamics", GMD Studies 85, GMD-FTT.

Brandt, A. (1998), "Barriers to achieving textbook multigrid efficiency in CFD", ICASE Interim Report 32, NASA CR-1998-207647, ICASE, NASA Langley Research Center, Hampton, VA.

Brandt, A., Diskin, B. and Thomas, J.L. (2002), "Recent advances in achieving textbook multigrid efficiency for computational fluid dynamics simulations", ICASE Report No. 2002-16, NASA/CR-2002-211656.

Briggs, W.L. (1987), *A Multigrid Tutorial*, SIAM, Philadelphia, PA.

Diskin, B. and Thomas, J.L. (2003), "New factorizable discretizations for the Euler equations", *SIAM J. Scientific Computing*, Vol. 25 No. 2, pp. 657-81.

Hackbusch, W. and Trottenberg, U. (Eds) (1982), *Multigrid Methods*, Lecture Notes in Math 960, Springer-Verlag, Berlin.

Mohamed, S.A., Mostafa, N.H., Matbuly, M.S. and Radwan, S.H. (2005), "Solution of incompressible Euler equation by an optimally efficient multigrid technique", *J. Engineering & Applied Science*, Vol. 52 No. 5, pp. 853-67.

Roberts, T.W., Sidilkover, D. and Swanson, R.C. (1997), "Textbook multigrid efficiency for the steady Euler equations", AIAA Paper 97-1949, pp. 97-1949.

Roberts, T.W., Sidilkover, D. and Tsynkov, S.V. (2002), "On the combined performance of nonlocal artificial boundary conditions with the new generation of advanced multigrid flow solvers", *Computer and Fluids*, Vol. 31, pp. 269-308.

Ta'asan, S. (1994), "Canonical-variables multigrid method for steady-state Euler equations", ICASE Report 94-14, NACA CR-194888.

Thomas, J.L., Diskin, B. and Brandt, A. (1999), "Textbook multigrid efficiency for the incompressible Navier-Stokes equations: high Reynolds number wakes and boundary layers", NASA/CR-1999-209831, ICASE Report No.99-51.

Wesseling, P. (1992), *An Introduction to Multigrid Methods*, Wiley, Chichester.

Wesseling, P. and Oosterlee, C.W. (2001), "Geometric multigrid with applications to computational fluid dynamics", *J. Computational and Applied Mathematics*, Vol. 128, pp. 311-34.

Corresponding author
S.A. Mohamed can be contacted at: s_a_Mohamed@hotmail.com